ELSEVIER

Journal of Nuclear Materials 278 (2000) 301–311

journal of nuclear materials

www.elsevier.nl/locate/jnucmat

Characterization of uranium corrosion products involved in a uranium hydride pyrophoric event

T.C. Totemeier

Argonne National Laboratory – West, P.O. Box 2528, Idaho Falls, ID 83402-2528, USA

Received 26 July 1999; accepted 13 September 1999

Abstract

Uranium metal corrosion products involved in a recent pyrophoric event were characterized using thermo-gravimetric analysis, X-ray diffraction, and BET gas sorption techniques to determine the effects of passivation treatment and long-term storage on chemical reactivity. Characterization was performed on corrosion products in three different conditions: immediately after separation from the source metal, after low-temperature passivation, and after passivation and extended vault storage. The hydride fraction and ignition temperature of the corrosion products were found to be strongly dependent on the corrosion extent of the source metal. There was little change in corrosion product properties resulting from low-temperature passivation or vault storage. The results indicate that the energy source for the pyrophoric event was a considerable quantity of uranium hydride present in the corrosion products, but the specific ignition mechanism could not be identified.

1. Introduction

The properties and behavior of uranium hydride (UH_3) formed as a product of the corrosion of U metal by water vapor are currently of interest due to the extended underwater storage of certain metallic spent nuclear fuels (SNF) and the anticipated long-term dry storage of SNF and U metal. Information on the oxidation and pyrophoric behavior of UH_3 is specifically needed for analyses of potential accidents involving corroded metal or SNF. The results of general characterization and oxidation testing of U metal corrosion products bearing significant fractions of UH_3 have recently been reported [1–3]. The products were collected from highly enriched uranium (HEU) metal fuel plates used in the Zero Power Physics Reactor (ZPPR) that corroded during extended vault storage.

A pyrophoric event involving similar corrosion products recently occurred at Argonne National Laboratory – West (ANL-W) [4]. The corrosion products had been passivated at room temperature and stored in air for a period of months. An extensive study of the corrosion products involved in the event was performed to help determine its cause. The study focused on determining changes in the chemical reactivity of the corrosion products due to room temperature passivation and extended storage in air. The effects of room temperature passivation and extended vault storage had not been previously quantified. The effect of source metal corrosion extent on corrosion product properties was also assessed. Limited previous testing [3] observed an effect of source metal corrosion extent on the reactivity of the corrosion products, with corrosion products from severely corroded plates showing greater reactivity than those from lightly corroded plates.

Chemical reactivity was measured using a thermogravimetric analyzer (TGA). Further characterization was performed using X-ray diffraction (XRD) and gas sorption analysis. XRD was used to measure the fractions of hydride and oxide phases present in the products, and gas sorption analysis was used to measure the specific surface areas of the products. This paper presents the results of the study and their implications with regard to the pyrophoric event and the passivation of UH_3 associated with SNF.

2. Background – pyrophoric event

The pyrophoric event involved corrosion products collected from HEU metal fuel plates used in ZPPR. The

0022-3115/00/$ - see front matter
PII: S0022-3115(99)00245-7

corrosion products, while nominally uranium oxide (UO_{2+x}), are known to bear a significant fraction of UH_3. The corrosion products formed during extended vault storage of the fuel plates over a 12-year period. The history of the ZPPR fuel plate corrosion problem and an initial characterization of the corrosion products is detailed in Refs. [1,2]. The unique storage configuration was the root cause of the severe corrosion – the U metal plates were tightly clad in stainless steel jackets with porous metal endplugs. The porous nature of the endplugs allowed access of ambient gas to the U, and the presence of the cladding created a crevice environment which supported the formation of UH_3 as a product of the reaction of water vapor with U metal.

In order to address the storage vulnerability of the plates and recycle the HEU present, a processing scheme for separation of useful U metal from the cladding and the corrosion products was developed and implemented. The procedure entailed decladding the plates in an inert atmosphere glovebox and separating the loose corrosion products from the metal coupons ('coupon' refers to an individual U metal piece, 'plate' refers to a clad assembly of two or more coupons). After separation, the metal coupons were collected and induction cast into a single large ingot.

The separated corrosion products underwent a passivation procedure intended to prevent pyrophoric events during subsequent handling and vault storage. In an Ar glovebox containing approximately 3% O_2, the products were ground into a fine powder using a mortar and pestle, spread into a thin layer, and exposed to the O_2-bearing environment for a minimum of 2 h. The products were then transferred to an enclosed air hood, where their passive nature was verified by vigorous agitation (stirring and pounding with a screwdriver). The products were then canned (quart-size food-pack type) for vault storage, with the intention that they would eventually be fully converted to oxide using a higher-temperature process.

After approximately one year of storage, it was desired to consolidate the corrosion products into fewer containers to conserve storage space in the vault. Individual cans were opened in an enclosed air hood and their contents poured into a large steel consolidation can. The contents of 13 food-pack cans were emptied into the consolidation can in this manner without incident. As the contents of the 14th can were poured into the consolidation can, the material from the 14th can began sparking. Flames quickly formed above the material in the consolidation can and in the 14th food-pack can.

Attempts to extinguish the fire using a commercial retardant containing sodium chloride and magnesium aluminum silicate (Met-L-X®, Ansul Fire Protection) were unsuccessful because a gas stream eminating from the burning powder in the consolidation can ejected the retardant. The fire eventually self-extinguished without damage to the hood or spread of contamination outside the hood. The full details of the event are presented in the formal investigation report [4].

An investigative team identified the direct cause of the event as a failure to passivate the corrosion products in at least one of the food-pack cans. However, the team could not conclusively identify the mechanism by which burning was initiated. Two possible scenarios were presented. The first was a thermal excursion scenario whereby the tall geometry of the consolidation can led to ignition by preventing adequate heat removal from slowly oxidizing powder in the can. In the second scenario, the 14th food-pack can was assumed to be the ignition source, implying that the material in this can was different than that in the previous 13 cans. Additional experiments were recommended to better understand the ignition mechanism and the nature of the corrosion products. The present study was performed in response to the recommendations.

3. Materials and procedures

3.1. Materials

The effects of room temperature passivation and long-term vault storage on corrosion product properties were evaluated by characterization of corrosion products in three different conditions. The variation in properties with source metal corrosion extent was determined for each condition by characterizing corrosion products obtained from a number of source plates. Descriptions of the products obtained for each condition are given below.

3.1.1. Unpassivated corrosion products

The first condition for which the properties of the corrosion products were measured was immediately after de-cladding of the plates and separation of the corrosion products from the metal coupons. A study of the corrosion products in this condition has been previously reported [3]. Additional unpassivated corrosion products were sampled and analyzed in the present study to better determine the effect of room temperature passivation on the corrosion product characteristics. Ten plates which showed moderate corrosion were selected and divided into two sets of five. The plates were de-clad in a glovebox with a pass-through Ar atmosphere, and the corrosion products collected from each set were combined into two separate 'batches'. The average corrosion extents of the source plates for the two batches were 1.16% and 1.41%. For this study, the corrosion extent is quantified as the mass of loose corrosion product divided by the total uranium mass of the plate or plates from which the corrosion products were col-

lected. For batches of corrosion products from multiple plates, this figure represents an average extent. A 2 g sample of the corrosion products in the unpassivated condition was taken from each batch immediately after decladding of the plates.

3.1.2. Passivated corrosion products

After initial sampling, the two batches of corrosion products were passivated. The O_2 content in the glovebox was increased to 3.5 vol% by admitting a small flow of air. The two batches were separately ground to a uniform powder using a mortar and pestle and then left to sit in the O_2-containing environment for 2 h. A second set of samples for TGA analysis was then taken from the passivated corrosion products.

3.1.3. Corrosion products after passivation and extended vault storage

Only 14 cans of corrosion products generated during the ZPPR fuel processing campaign were involved in the pyrophoric event, and 21 cans of nearly identical material remained in the vault. This material was collected from source plates with a broad range of corrosion extents, and hence the effect of corrosion extent could be readily quantified for this condition. TGA tests to measure the ignition temperature and hydride fraction of the vault-stored products were performed on samples from every can; XRD and BET analyses were performed on samples from selected cans.

3.2. Analysis procedures

3.2.1. Gas sorption analysis

BET gas sorption analysis was performed on corrosion products in the vault-stored condition to compare their specific surface areas with those obtained for unpassivated powders in the earlier study [3]. The specific surface area is also a required parameter for analysis of the oxidation kinetics measured in a TGA test. Analysis was performed using a Quantachrome Quantasorb® analyzer and standard BET techniques with Kr gas as the adsorbate, He gas as the carrier, and N_2 gas for calibration. Adsorption was carried out at liquid N_2 temperature; three consecutive measurements were made on each sample. The test matrix and results are shown in Table 1.

Table 1
BET results summary

Material	Corrosion extent[a] (%)	Specific surface area (m^2/g)
Unpassivated product		
Plate 2249	0.64	0.50–0.52
Plate 3411	1.08	0.74–0.76
Plate 2962	1.53	0.95–1.04
Plate 3930	1.67	0.76–0.77
Plate 3401	1.83	0.73–0.78
Plate 2652	1.98	0.75–0.80
Vault-stored product		
SB97-1	0.33	0.93
BWHEU-F-IC008	0.85	0.76–0.79
RAM97-9/10	1.07	0.71–0.76
RAM97-23/24	1.80	0.83–0.84
BWHEU-F-IC009	1.83	0.89–0.99

[a] Defined as mass of corrosion product divided by total uranium mass.

3.2.2. Oxidation testing

A modified Shimadzu TGA-51H analyzer located in a purified Ar glovebox was used to measure the oxidation kinetics and hydride content of the corrosion product powders. Details of the testing apparatus and analysis techniques are presented in Ref. [3]. The standard test performed was the burning curve test, in which a 200 mg sample is heated at 15°C/min in a flowing Ar–20% O_2 atmosphere while the sample weight and furnace control thermocouple temperature are monitored. Ignition of the sample is clearly indicated by a sharp, simultaneous increase in both values; the ignition temperature is defined as the furnace temperature at this point. The sample is oxidized to completion, indicated by a stable sample weight. For samples which are known to contain UH_3, the total weight change during burning is used to calculate the fraction of UH_3 in the sample via the stoichiometry of the UH_3–O_2 reaction. Table 2 is a summary of the burning curve test results.

Isothermal oxidation tests were also performed. In an isothermal test, the sample is heated to the test temperature in a pure Ar atmosphere. When the test temperature is reached and stabilized, an Ar–30%O_2 reacting gas is admitted into the sample chamber by opening a solenoid valve in its supply line. Mixing of the reacting gas with a pure Ar purge gas reduces the O_2 concentration in the sample chamber to 20%. The weight of the sample is recorded for the duration of the test. Isothermal oxidation tests performed in this investigation were typically 300 or 600 min long.

Isothermal testing was performed on samples of vault-stored corrosion product for two purposes – to enable a comparison of low-temperature reaction rates with those previously measured for unpassivated products, and as a simulation of the passivation process. In the latter case, it was originally hypothesized that reaction of the hydride-bearing corrosion products with O_2 would reduce their reactivity by the formation of a passive oxide film on the surface of the hydride. This was the principle on which the original passivation scheme was based. To better test the hypothesis, corrosion product samples were first isothermally reacted with O_2

Table 2
Summary of corrosion product reactivity characteristics

Material	Total U wt (g)	Corrosion product wt (g)	Corrosion extent (%)	UH_3 content[a] (%)	Ignition Temp. (°C)
Unpassivated product					
Plate 2249	222	1.42	0.64	N/A[b]	N/A[b]
Plate 3411	222	2.40	1.08	17–19	144–166
Batch 1	1104	12.86	1.16	N/A	N/A
Batch 2	1108	15.62	1.41	13–15	145–166
Plate 3401	220	4.04	1.83	47–61	142
Plate 2652	220	4.35	1.98	29–39	134–137
Passivated product					
Batch 1	1104	12.86	1.16	N/A	N/A
Batch 2	1108	15.62	1.41	18	159–161
Vault-stored product					
SB97-1	5747	19.07	0.33	N/A	N/A
RAM97-32/33	11 469	43.86	0.38	N/A	N/A
RAM97-30/31	11 492	50.62	0.44	N/A	N/A
RAM97-28/29	11 489	54.42	0.47	N/A	N/A
RAM97-21/22	11 737	89.06	0.76	4–5	190–215
RAM97-25	5893	48.95	0.83	N/A	N/A
BWHEU-F-IC008	5948	50.50	0.85	N/A	N/A
RAM 1-2	7947	72.81	0.92	N/A	N/A
RAM 3-4	8996	83.42	0.93	N/A	N/A
RAM97-17/18	11 801	114.91	0.97	10–11	171–183
RAM97-22/23	11 739	120.60	1.03	N/A	N/A
RAM97-9/10	11 746	125.87	1.07	14–17	159–166
RAM97-5/6	11 737	129.68	1.10	17–18	154–164
RAM97-7/8	11 746	140.71	1.20	11	176–181
RAM97-33/34	11 735	141.51	1.21	12–13	166–174
RAM97-13/14	11 789	151.64	1.29	18–21	153–155
RAM97-11/12	11 761	153.26	1.30	15–18	153–155
RAM97-19/20	11 790	177.93	1.51	15–16	161–167
RAM97-23/24	11 736	210.83	1.80	22–25	153–157
BWHEU-F-IC009	11 694	214.50	1.83	27–29	160–166

[a] Calculated from weight gain after complete oxidation.
[b] N/A – Material did not ignite in burning curve tests.

below the ignition temperature, then cooled to room temperature and tested in a burning curve mode. An increase in ignition temperature after isothermal oxidation testing would indicate a passivation effect. The effect of low-temperature passivation was also assessed by testing of corrosion products before and immediately after passivation, as described in Section 3.1.2.

3.2.3. X-ray diffraction

XRD was used for identification of metal, oxide, and hydride phases present in the corrosion product samples. The XRD test matrix and results are shown in Table 2. For samples that contained hydride, standardless analysis was performed using Sietronics phase analysis software to quantify the fractions of hydride and oxide for comparison with the results of the TGA tests. Samples for XRD analysis were taken from the same corrosion product samples that were used for TGA testing. All XRD samples were crushed to a fine powder in a high-purity Ar glovebox and loaded into a sealed environmental chamber. The loaded chamber was transferred out of the glovebox to the diffractometer. Diffraction was performed on a Scintag X1 powder diffractometer using Cu K-α radiation.

4. Results

4.1. Specific surface areas

The results of the BET specific surface area analyses are shown in Table 1. The data for unpassivated corrosion products are taken from Ref. [3]. In the present investigation, BET analysis was performed only on samples of vault-stored corrosion products. The specific surface areas of the vault-stored products were essen-

tially identical to those of the unpassivated products. The specific surface areas for all samples fell within the range 0.5–1.0 m^2/g, with the majority of the values approximately 0.7–0.8 m^2/g. There was no effect of corrosion extent on specific surface area.

4.2. Burning curve reactivity

Table 2 summarizes the results of burning curve tests performed on unpassivated, passivated, and vault-stored material. The entries in Table 2 are sorted by material condition and sub-sorted by corrosion extent. Each entry corresponds to the results from 2 or 3 individual tests. Data for individual unpassivated plates are from Ref. [3].

Fig. 1 shows a typical burning curve plot for a test in which ignition occurred. The sharp increases in sample weight and furnace control thermocouple reading at ignition are clearly visible. The sample weight plateaus after burning is complete; the increase in weight to this initial plateau was used to compute the hydride fraction. Most burning curve tests were terminated when the first plateau was reached. If the test was not terminated at the initial plateau, a second increase in sample weight was observed, at a temperature of approximately 400°C. This higher-temperature weight gain consistently occurred for all materials and is believed to correspond to oxidation of UO_{2+x} originally present in the sample to U_3O_8. As described below, XRD analyses of samples after testing to high temperatures showed only U_3O_8, while samples terminated immediately after burning still showed UO_{2+x}.

Fig. 2 shows a typical burning curve plot for a test which did not show ignition. There is an initial weight loss believed to correspond to water vapor desorption. At approximately 200°C the weight gradually increases, but ignition does not occur. The change in weight is not dramatic (compare to Fig. 1), and there is no deviation of the furnace temperature from the preset rate. The rate of weight increase slows at 300°C and then re-accelerates at approximately 400°C. This second weight gain occurs at the same temperature as the second weight gain in tests which did ignite and is also believed to correspond to oxidation of UO_{2+x} to U_3O_8.

Figs. 3 and 4 are plots of hydride fraction and ignition temperature as a function of corrosion extent for all conditions. There is considerable scatter, but ignition consistently occurred for corrosion extents above 1.2% and consistently did not occur for corrosion extents below 0.7%. For samples which ignited, the hydride

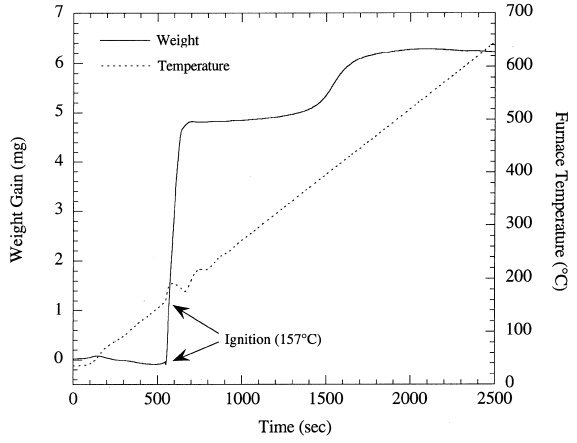

Fig. 1. Typical burning curve plot for TGA test in which ignition occurred (FMFVLT 15, vault-stored corrosion product).

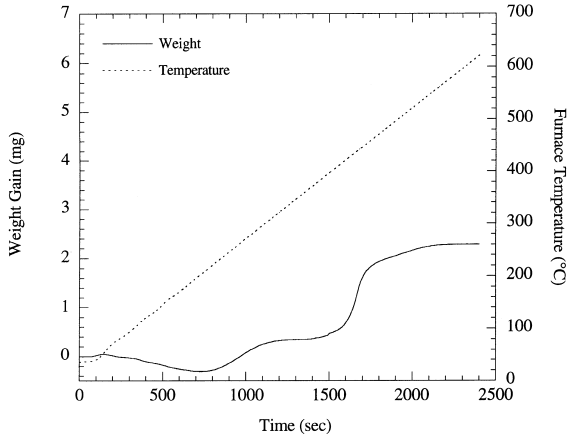

Fig. 2. Typical burning curve plot for TGA test in which ignition did not occur (FMFVLT 06, vault-stored corrosion product).

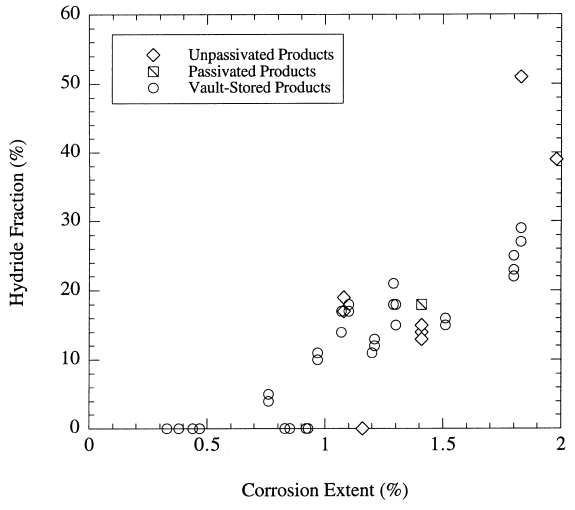

Fig. 3. Plot of TGA hydride fraction versus corrosion extent for ZPPR corrosion products. Data points with an ignition temperature of zero did not ignite.

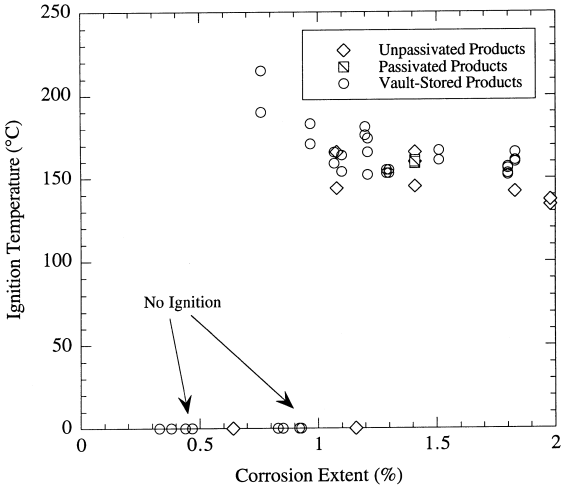

Fig. 4. Plot of ignition temperature versus corrosion extent for ZPPR corrosion products. Data points with an ignition temperature of zero did not ignite.

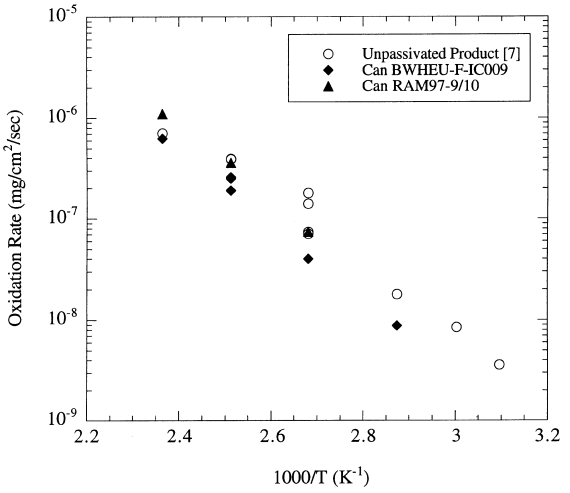

Fig. 5. Plot of isothermal oxidation rates versus reciprocal temperature for ZPPR corrosion products.

fraction is roughly linearly dependent on corrosion extent. Ignition temperature is less strongly dependent on corrosion extent. Ignition temperature decreases with increasing corrosion extent to 1.2%, but is relatively independent of corrosion extent above 1.2%.

As shown in Figs. 3 and 4, there is little difference in hydride fraction or ignition temperature between the three different corrosion product conditions. For both parameters, the data for the three conditions fall within the same scatterband. The lack of change in properties due to passivation is additionally demonstrated by comparing data for corrosion products from Batch 2 before and after passivation (Table 2).

4.3. Isothermal oxidation kinetics

Fig. 5 is an Arrhenius plot of oxidation rates versus reciprocal temperature for isothermal tests on unpassivated and vault-stored corrosion products. Tests were performed on corrosion products from two cans with different corrosion extents. The oxidation rates shown are best linear fits to weight gain versus time data for each test normalized by reacting surface area, as described in Ref. [3]. The shapes of the weight gain versus time curves for tests on the vault-stored products were similar to those for tests on unpassivated products, i.e. the rate of weight gain slowly decreased throughout each test. The UH_3 surface area used to normalize the weight gain data was computed as the product of the BET specific area, the sample mass, and the hydride fraction. The calculation assumes that the oxide and hydride components of the corrosion product have the same specific area. The basis for this assumption is presented in Ref. [3].

There was no significant difference in the oxidation rates measured for the two material conditions. The data for the two cans of vault-stored corrosion products lie within the scatterband for the unpassivated products. The rate equation for the unpassivated material is

$$k = 67\exp(63\,000/RT)\ \mathrm{mg/cm^2/s}, \quad (1)$$

where k is the normalized linear rate constant, and R is the gas constant in units of J/K/mol. The rate equation for the vault-stored corrosion products is

$$k = 1380\exp(74\,000/RT)\ \mathrm{mg/cm^2/s}. \quad (2)$$

Although the pre-exponential factors and activation energies for the two conditions are different, the difference does not have statistical significance due to the scatter in the data.

The effect of pre-oxidation on subsequent burning curve reactivity was assessed by performing burning curve tests on partially oxidized samples from the isothermal tests. The results of these tests are presented in Table 3. Significant pre-oxidation resulted in an increase in ignition temperature. For material from can BWHEU-F-IC009, the ignition temperature increased from 160°C to 208°C as a result of oxidation at 150°C. A similar increase was observed for material from can RAM97-9/10. The magnitude of the ignition temperature increase depended on the extent of pre-oxidation. Little increase was observed when the weight gain incurred in the isothermal test was low.

4.4. X-ray diffraction

Table 4 summarizes the results of the XRD analyses. The phases identified in each sample are listed. For

Table 3
Results of burning curve tests on pre-oxidized vault-stored ZPPR corrosion products

Test	Material	Pre-oxidation conditions			$T_{ignition}$ (°C)	$\Delta T_{ignition}$ [a] (°C)
		Temp. (°C)	Time (min)	%UH_3 reacted		
FMFVLT76	BWHEU-F-IC009	50	600	1.5	151	−12
FMFVLT78	BWHEU-F-IC009	75	600	3.1	173	+10
FMFVLT72	BWHEU-F-IC009	100	600	14	180	+17
FMFVLT63	BWHEU-F-IC009	125	240	23	181	+18
FMFVLT65	BWHEU-F-IC009	125	240	24	159	−4
FMFVLT67	BWHEU-F-IC009	125	480	38	188	+25
FMFVLT74	BWHEU-F-IC009	150	240	66	208	+45
FMFVLT84	RAM97-9/10	50	600	0[b]	169	+6
FMFVLT80	RAM97-9/10	100	600	8.0	183	+20
FMFVLT82	RAM97-9/10	125	600	19	187	+24
FMFVLT86	RAM97-9/10	150	300	62	214	+51

[a] Difference from average baseline ignition temperature for corresponding material shown in Table 2.
[b] No measurable weight gain.

Table 4
XRD results summary

Material	Corrosion extent (%)	Phases identified	Wt% UH_3 (XRD)	Wt% UH_3 (TGA)
Unpassivated product				
Plate 2249	0.64	UO_{2+x}[a], UH_3	3	No ignition
Plate 2652	1.98	UO_{2+x}, UH_3	47	29–39
Vault-stored product				
SB97-1	0.33	UO_{2+x}, UH_3	4	No ignition
RAM97-21/22	0.76	UO_{2+x}, UH_3	9	4–5
BWHEU-F-IC008	0.85	UO_{2+x}, UH_3	4	No ignition
RAM97-1/2	0.92	UO_{2+x}, UH_3	4	No ignition
RAM97-9/10	1.07	UO_{2+x}, UH_3	18	14–17
RAM97-23/24	1.80	UO_{2+x}, UH_3	26	22–25
BWHEU-F-IC009	1.83	UO_{2+x}, UH_3	42	27–29
Vault-stored product after burning curve testing				
BWHEU-F-IC008 Oxidized to 620°C	0.85	U_3O_8	N/A	N/A
BWHEU-F-IC009 Oxidized to 250°C	1.83	UO_{2+x}, major U_3O_8, minor	N/A	N/A
Burned product				
Sample 2	N/A	UO_{2+x}, major NaCl, U_3O_8, minor	N/A	No ignition
Sample 3	N/A	UO_{2+x}, major NaCl, U_3O_8, minor	N/A	No ignition

[a] UO_{2+x} denotes oxide which may be UO_2, U_3O_7, or a mixture of both.

samples which contained oxide and hydride, the result of the quantitative analysis of the XRD pattern is shown, with the corresponding TGA result for comparison. For samples containing phases other than oxide and hydride, the major and minor peaks of the pattern are identified. Hydride peaks were observed for all unpassivated and vault-stored samples, even for those which did not ignite in TGA testing. The quantitative analysis results showed a dependence of UH_3 content on corrosion extent similar to that observed in TGA tests. The samples which did not ignite in TGA testing showed low hydride fractions in the XRD analysis.

No UH_3 was observed in the post-test XRD pattern of a TGA sample from can BWHEU-F-IC009. After ignition and burning to the initial plateau in weight at 250°C, the sample showed peaks from both UO_{2+x} and U_3O_8. TGA oxidation of a sample from can BWHEU-F-IC009 to 620°C resulted in the conversion of lower

oxides originally present in the sample to U_3O_8. The UH_3 originally present in this sample was also reacted.

5. Discussion

5.1. Effect of corrosion extent on properties

5.1.1. Specific surface area

There was no effect of corrosion extent on the specific surface areas measured for unpassivated and vault-stored corrosion products. The specific surface areas were generally between 0.7 and 1.0 m^2/g, regardless of corrosion extent. Only one outlier from this range is present, at 0.5 m^2/g for a corrosion extent of 0.64%. The lack of an effect of corrosion extent on specific area was discussed in Ref. [3]. Because of the relatively constant specific area, this parameter did not correlate with the observed variations in ignition temperature, as is commonly observed for U metal [5].

5.1.2. Chemical reactivity

The ignition temperature and hydride fraction of the corrosion products were found to be strongly dependent on source metal corrosion extent. These effects are shown in Table 2 and Figs. 3 and 4. The dependence of hydride fraction on extent is a result of variations in the amount of localized corrosion for different plates. As documented in Ref. [1], the hydride component of the corrosion products (a black powder) tends to be associated with areas of severe localized corrosion, while light gray oxide flakes are associated with general corrosion. Plates with more localized corrosion (more hydride) tend to have a greater corrosion extent. Plates which do not have any areas of localized corrosion (and hence little hydride) typically have only a small amount of corrosion product (low corrosion extent).

The results of the XRD analyses of the corrosion products support the TGA findings. Reasonable agreement was found between hydride fractions computed using the weight gain in TGA tests and those computed using the XRD standardless quantitative analysis software. Some differences did exist – the values from XRD analysis were typically higher than from TGA analysis, and XRD detected the presence of hydride for all unpassivated and vault-stored corrosion products, even for those samples which did not ignite in TGA tests. The source of the discrepancy between the values obtained with the two techniques is currently unknown. The small quantity of UH_3 detected in X-ray analysis is believed to be the source of the weight gain observed at approximately 200°C in TGA tests that did not show ignition.

The effect of corrosion extent on ignition temperature is related to its effect on hydride fraction. Ignition is defined by a balance between heat generation and loss; the strong dependence of oxidation rates on temperature results in rapid self-heating when the rate of heat generation due to oxidation exceeds the rate of heat loss. Samples with higher hydride fractions have a greater heat generating capacity relative to the total mass of the sample, and so are expected to ignite at lower temperatures than samples with low fractions. Samples with very low hydride fractions may not ignite at any temperature, since the small amount of heat generated by oxidation of the hydride can be absorbed by a large quantity of intimately surrounding oxide.

The variation of ignition temperature with hydride fraction for samples which ignited is shown in Fig. 6. Ignition was not observed for hydride fractions less than 4%. Above 4% hydride, the ignition temperature decreases relatively quickly with increasing hydride fraction until 15% is reached, then decreases much more slowly (if at all) for hydride fractions greater than 15%. A possible explanation for the relative independence above 15% is that sufficient hydride is present that the ignition temperature is determined more by the intrinsic oxidation kinetics of the hydride than the inert nature of the oxide. Numerical modeling has been initiated to better understand the ignition process for this material.

Fig. 4 shows inconsistent ignition behavior in the region between 0.7% and 1.2% corrosion extent. Some samples did not ignite, while others ignited and followed the trends in ignition temperature shown by samples with higher extents. The inconsistent behavior may be a result of plates with similar overall corrosion extent having varying hydride fractions. The scatter in hydride content at a given corrosion extent is fairly large, as shown in Fig. 3. Therefore, for lower corrosion extents, some corrosion products may have sufficient hydride for ignition and some may not.

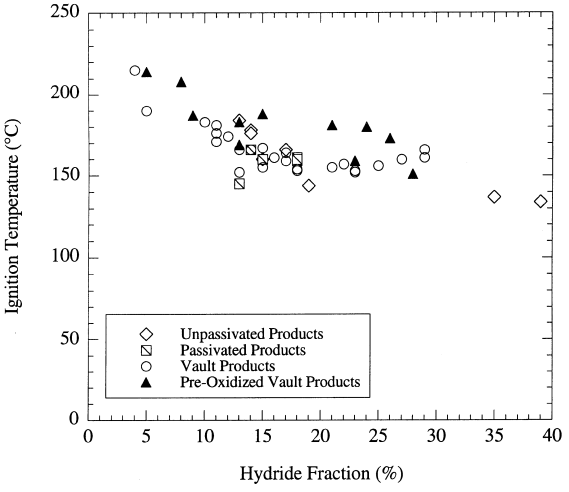

Fig. 6. Plot of ignition temperature as a function of hydride fraction for ZPPR corrosion products.

No effect of corrosion extent was observed for isothermal oxidation data below the ignition temperature. The data from corrosion products with four different corrosion extents (two plates and two vault-stored cans) fall into essentially the same scatterband in Fig. 5. Because the data presented in Fig. 5 has been normalized by hydride surface area, the effect of varying hydride fraction is accounted for. There is therefore no intrinsic variation in low-temperature oxidation rate with corrosion extent. There is also no significant effect of storage condition.

5.2. Changes in properties due to passivation and storage

Given the dependence of corrosion product properties on corrosion extent described above, any evaluation of changes in properties due to passivation and storage must account for corrosion extent. This is accomplished by comparing data from different conditions on plots of properties versus corrosion extent, where a significant difference is manifest as an outlying data point or curve. The data shown in Figs. 3 and 4 demonstrate the similarity of properties for unpassivated, passivated, and vault-stored corrosion products. All conditions fall into the same broad scatterband. The lack of an effect of the room-temperature passivation process on the ignition temperature or hydride fraction is confirmed by the results obtained from the two batches of corrosion product tested before and immediately after passivation.

The lack of an effect of passivation and storage is consistent with the low-temperature oxidation rates measured for the corrosion products. The room temperature oxidation rate is so slow that it is difficult to measure using the TGA apparatus. The extrapolated rate at 25°C using Eq. (1) is 6×10^{-10} mg/cm^2/s. A 1% extent of reaction requires 80 h at this rate, assuming a specific surface area of 1 m^2/g and 20% hydride. Therefore, exposure of the corrosion products to oxygen for 2 h in the passivation step reacts an insignificant quantity of UH_3. Grinding during the passivation step has the potential to accelerate oxidation by crushing UH_3 particles and exposing fresh surfaces, but this effect is apparently not significant since there are no indications of reduced hydride fraction.

The longer duration of vault storage is expected to result in a greater extent of reaction, but the experimental data do not indicate that the vault-stored material has a significantly lowered hydride fraction relative to the unpassivated condition. The lack of reaction is likely due to limitation of O_2 supply to the corrosion product, as the storage cans are sealed. In addition, the decreasing rate of oxidation observed in TGA tests could result in much lower long-term oxidation rates than those measured over relatively short durations in the TGA.

The results of the burning curve tests on pre-oxidized, vault-stored corrosion products demonstrate that partial reaction of hydride does raise the ignition temperature. However, a large fraction of the hydride must be reacted, and the change in ignition temperature is relatively small. In the extreme case (test FMFVLT 86), reaction of 62% of the hydride present in the sample increased the ignition temperature by only 51°C, from the baseline value of 163°C to 214°C (Table 3). Reaction of lower fractions (~20%) increased the ignition temperature less than approximately 20°C.

The increase in ignition temperature resulting from significant pre-oxidation can be accounted for by the reduction in hydride fraction. Reaction of hydride in an isothermal oxidation test lowers the net hydride fraction for the subsequent burning curve test. As shown in Fig. 6, ignition temperature increases with decreasing hydride fraction, especially for fractions less than 15%. The data for pre-oxidized material are highlighted with solid markers. The hydride fractions for these samples were computed using only the weight gains which occurred in the burning curve tests. The data for the pre-oxidized samples generally fall within the scatterband of the other data (although some points lie at the upper bound), demonstrating that the increase in ignition temperature resulting from pre-oxidation is primarily due to the lowered hydride fraction rather than another passivation effect.

The lack of an effect of the low-temperature passivation step and results obtained in pre-oxidation tests indicate that true passivation – a significant reduction in reactivity due to formation of a thin, passive layer of oxide on the surface of a hydride particle – does not appear to occur for ZPPR corrosion products. Formation of such passivating films has been indicated to lower the reactivity of UH_3 powders formed by reaction with H_2 gas [6,7]. Passivation may not appear to occur for the ZPPR corrosion products because the UH_3 present is likely already passivated due to its formation in an oxidation process (as opposed to reaction with pure H_2 gas) and the intimate presence of oxide and water vapor. The similarity of ZPPR corrosion product ignition temperatures to those reported for 'passivated' UH_3 by Longhurst, 140°C [6], supports this argument. Hydride associated with other uranium metal corrosion products, i.e. on metallic spent nuclear fuels, would be expected to be similarly passivated. However, the experience with ZPPR corrosion products demonstrates that 'passivated' UH_3 with ignition temperatures exceeding 100°C may still ignite at room temperature under certain handling conditions.

5.3. Sources and mechanisms for the pyrophoric event

Another issue that this study addressed is the cause of the pyrophoric event and the specific mechanism of

ignition. The energy source is clear – the corrosion products contained a substantial quantity of UH_3 which reacted with air in the event. The ignition temperature of the corrosion products was essentially the same as immediately following removal from the source plates; the material was not at all passivated relative to its initial condition. The specific mechanism by which ignition of the corrosion products occurred still cannot be conclusively identified. However, the data obtained in this series of tests can be used to analyze the mechanisms proposed by the investigative team – the thermal excursion scenario and the can 14 scenario [4].

In the thermal excursion scenario, oxidation slowly increases the temperature of the consolidated product to the ignition point because the tall cylindrical can prevents effective heat loss from the powder. Simple analysis using low-temperature oxidation data obtained for the unpassivated and vault-stored corrosion products shows this scenario to be extremely unlikely. As mentioned in Section 5.2, the rate of oxidation for the corrosion products at 25°C is 6×10^{-10} mg/cm^2/s. There were 1.77 kg of corrosion product in the consolidation can. For conservative values of specific area (1.0 m^2/g) and hydride fraction (20%), adiabatic heating due to oxidation results in a temperature increase of 2×10^{-5} K/s. At this rate of increase, 13 h are required for the powder to heat one degree. Since the consolidation operation was performed in less than 4 h, the corrosion product could not have self-heated to the ignition point (at least 130°C). The thermal excursion scenario is therefore not plausible.

The second proposed scenario was that in which the 14th can was different than the previous 13. Three possibilities were presented: (1) the material in the 14th can was fundamentally different; (2) the material in the 14th can was improperly passivated; and (3) the material in the 14th can had changed (become more reactive) during storage. The results of this study indicate that there was no effect of the passivation step. Therefore, the material in can 14 could not have been inadequately passivated relative to the other cans. The results also indicate that an increase in reactivity did not occur as a result of storage. The material in can 14 was different, however, in that it was collected from source plates with a corrosion extent (1.8%) higher than any of the previous 13 cans. Therefore, can 14 likely had an ignition temperature lower than the other 13 cans, and a higher pyrophoric potential.

Operator observations of the event indicated that the fire indeed appeared to initiate in the can 14 material, but the ignition source remains unidentified. Two possible 'sparks' are static discharge or mechanical agitation during pouring of the powder. Also, the question of why the material did not ignite during stirring and handling in air prior to vault storage remains unanswered. This experience highlights the unpredictable nature of UH_3. The only way to insure safety during handling of hydride-bearing powders is to perform all operations in inert environments or to fully convert the hydride by controlled oxidation at high temperature.

6. Conclusions

Hydride-bearing uranium metal corrosion products from ZPPR fuel plates involved in a pyrophoric event at ANL-W were characterized using TGA, XRD, and BET techniques. The following conclusions were reached:

1. The hydride fraction of corrosion products increased with increasing corrosion extent of the source plates. The ignition temperature of the corrosion products decreased with increasing corrosion extent and hydride fraction.
2. There was little change in corrosion product properties after passivation or long-term vault storage. The passivation step did not alter either the ignition temperature or the hydride fraction of the corrosion products.
3. Partial oxidation of the corrosion products, decreased reactivity by increasing the ignition temperature, but a large reaction extent was required to achieve only a small increase in ignition temperature. Therefore, complete oxidation of the hydride is required to guarantee safe handling and storage.
4. The energy source for the pyrophoric event was a considerable quantity of UH_3 present in the corrosion products. No specific ignition mechanism could be conclusively identified, but the available evidence disproves a scenario in which the powder in the consolidation can slowly self-heated to the ignition point. The experience highlights the unpredictable nature of UH_3.

Acknowledgements

The author wishes to acknowledge R.J. Briggs, E.A. Belnap, and R. Gonzales for their work in sampling the ZPPR corrosion products, S.M. Frank for performing the XRD analyses, and R.G. Pahl for helpful advice and review of this report. This work was supported through funding by the US Department of Energy, Reactor Systems, Development and Technology, under contract W-31-109-Eng-38.

References

[1] T.C. Totemeier, R.G. Pahl, S.L. Hayes, S.M. Frank, J. Nucl. Mater. 256 (1998) 87.
[2] T.C. Totemeier, R.G. Pahl, S.L. Hayes, S.M. Frank, Metallic uranium ZPPR fuel: corrosion characteristics and corrosion product oxidation kinetics, Argonne National Laboratory Report ANL-98/11, 1998.

[3] T.C. Totemeier, R.G. Pahl, J. Nucl. Mater. 265 (1999) 308.
[4] U.S. Department of Energy ORPS Investigation Report CH-AA-ANLW-FMF-0001, Argonne National Laboratory – West site uranium corrosion product fire March 13, 1998.
[5] L. Baker Jr., J.G. Schnizlein, J.D. Bingle, J. Nucl. Mater. 20 (1966) 22.
[6] G.R. Longhurst, Pyrophoricity of tritium-storage bed materials, EG & G Idaho Report EGG-FSP-8050, 1988.
[7] S.L. Robinson, G.J. Thomas, Uranium hydride formation and properties: a review with commentary on handling and disposition, Sandia National Laboratory Report SAND96-8206, 1996.